

Cite this: *CrystEngComm*, 2012, **14**, 3424

www.rsc.org/crystengcomm

PAPER

Self-assembly of seven diamide-containing pyridinium salts *via* nonconventional C–H···O hydrogen bonding catemers†

An-Kai Wu and Kwang-Ming Lee*

Received 30th October 2011, Accepted 8th February 2012

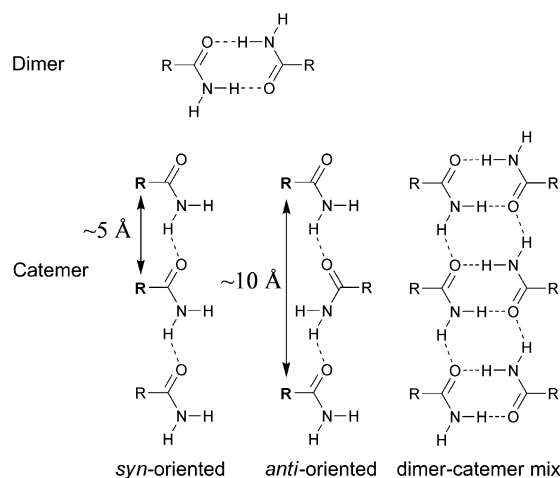
DOI: 10.1039/c2ce06448k

A series of 1-(2-amino-2-oxoethyl)-3-carbamoylpyridin-1-ium salts with different anions (Cl^- , Br^- , BF_4^- , NO_3^- , OTf^- , PF_6^- and BPh_4^-) have been synthesized and characterized by single crystal X-ray diffraction. The results demonstrate that the L-shaped diamide pyridinium cations can aggregate convergently to form a tubular structure or divergently to form a one-dimensional ribbon structure or two-dimensional brick, grid and sheet structures *via* different hydrogen bonding catemer motifs, including conventional N–H···O type (BPh_4^- (7)), the nonconventional N–H···O types (Cl^- (1)) and, the mixed N–H···O/C–H···O type (OTf^- (5) and PF_6^- (6)), and the interesting pure C–H···O types (Cl^- (1), Br^- (2) and BF_4^- (3)).

Introduction

Nonconventional C–H···X (X = O, N and anions) hydrogen bonding^{1–6} has received attention due to its importance in supramolecular structures,^{7–18} biological structures,^{19–27} and anion receptors.^{28–33} Although the structural characteristics of C–H···X interactions are relatively well documented, the role of the C–H···X hydrogen bond in crystal packing is still not clear, especially the roles that C–H···X hydrogen bonds play when they coexist with other conventional, strong, hydrogen bonding groups, such as amide, carboxylic acid and ester groups. For example, the C–H group exists in the presence of these other strong hydrogen bonding groups in amino acids, proteins, protein–ligand complexes and acyl-enzyme species.³⁴ Therefore, it would be helpful to investigate C–H···X hydrogen bonding by using small molecules to simplify the system. For example, using charge-enhanced C–H donor cationic molecules would increase the proton donor ability of the C–H moiety, and a series of weak or strong hydrogen bond acceptors, such as carbonyl groups or X^- anions, would aid in the investigation of the competition for weak hydrogen bonding between these hydrogen bond acceptors and the associated hydrogen bond donors. Meanwhile, it is helpful to understand how the anions tune the hydrogen bonding interactions involving the cationic moieties within the C–H donor-rich environment of the crystal structure. In fact, anionic species play important roles in biological structures, supramolecular chemistry and crystal engineering due to the great variety of their shapes, sizes, charges and basicities. The primary amide group (–C(=O)NH₂) with intermolecular N–H···O hydrogen

bonding is a well known supramolecular synthon in crystal engineering.³⁵ Generally, there are four possible amide hydrogen bonding motifs, including the simple dimer, the *syn*- and *anti*-oriented N–H···O catemers and a dimer–catemer mixed motif (Scheme 1).³⁶ Recently, we reported a series of pyridinium salts with both *N*-acetamido and ethyl acetate functional groups.³⁷ The L-shaped cations could form well-defined structures *via* different synthons. The conventional N–H···O hydrogen bonding dimer or catemer motifs could be formed only when the anions were BF_4^- or PF_6^- , but these motifs were disturbed when Br^- or OTf^- were used. In other words, the results demonstrated that the amide motifs are significantly affected by the hydrogen bonding acceptor abilities of the anionic species. Here, we report the subsequent results achieved by changing the ethyl acetate to



Scheme 1 Conventional amide hydrogen bonding dimer and catemer motifs and the space requirement for the R groups.

Department of Chemistry, National Kaohsiung Normal University, 62, Shen-Shung Road, Kaohsiung 824, Taiwan. E-mail: kmlee@nknmu.edu.tw; Fax: +886-7-6051083; Tel: +886-7-7172930 ext 7119

† CCDC reference numbers 838304–838310. For crystallographic data in CIF or other electronic format see DOI: 10.1039/c2ce06448k

an amide group to form a series of diamide-functionalized pyridinium salts with seven anions, including Cl^- , Br^- , BF_4^- , NO_3^- , OTf^- , PF_6^- and BPh_4^- .

The results demonstrate that the different types of hydrogen bonding catemer motifs formed in six salts except the NO_3^- salt; however, the conventional pure $\text{N-H}\cdots\text{O}$ hydrogen bonding catemer is formed only in the BPh_4^- salt. When the anions are Br^- and BF_4^- , the conventional $\text{N-H}\cdots\text{O}$ hydrogen bonding catemers are disturbed, and the pure $\text{C-H}\cdots\text{O}=\text{C}$ type catemers are formed instead. However, in the structures of Cl^- , OTf^- and PF_6^- salts, the mixed $\text{C-H}\cdots\text{O}/\text{N-H}\cdots\text{O}$ types of hydrogen bonding catemers are observed. From these catemer and dimer motifs, the different packing structures, including tubular, ribbon, brick and sheet-like structures, form depending on the shapes and sizes of the anion species. This study will help clarify how the amide motifs and the packing structures of the diamide-containing cationic molecules are affected by different anion species, and it provides useful information for the application of these motifs in the field of crystal engineering.

Experimental

General materials and methods

The 1-(2-amino-2-oxoethyl)-3-carbamoylpyridin-1-ium chloride (**1**) and bromide (**2**) salts were synthesized first by the reaction of nicotinamide with 2-chloroacetamide and 2-bromoacetamide, respectively. The BF_4^- (**3**), NO_3^- (**4**), OTf^- (**5**), PF_6^- (**6**), and BPh_4^- (**7**) salts were obtained by the reaction of **1** with AgBF_4 , AgNO_3 or AgOTf or by the metathesis reactions with NH_4PF_6 or NaBPh_4 salts, respectively.

1-(2-Amino-2-oxoethyl)-3-carbamoylpyridin-1-ium chloride (1). A solution of nicotinamide (2.0034 g, 16.40 mmol) and 2-chloroacetamide (1.5953 g, 17.06 mmol) was refluxed in acetonitrile for 32 h. After cooling, the white-yellow precipitated powder was collected and recrystallized from H_2O /methanol (1 : 3) solution *via* layering with diethyl ether to give the product **1** with a yield of 2.9385 g (13.63 mmol) or 83%. Column-shaped crystals suitable for single crystal X-ray diffraction were obtained by recrystallization of the product (0.1103 g) from a H_2O (1 ml)–DMF (7 ml) mixed solution *via* vapor diffusion of THF. $^1\text{H-NMR}$ (300 MHz, d^6 -DMSO, ppm): 9.56 (s, 1H, $-\text{N-CH-CCO-}$), 9.13–9.11 (d, 1H, $^3J = 7.2$ Hz, $-\text{N-CH-CH-}$), 9.11–9.08 (d, 1H, $^3J = 9.5$ Hz, $-\text{CH-CH-C-CO-}$), 8.82, 7.72 (s, 1H, N-CH-C-CO-NH_2), 8.29–8.24 (t, 1H, $^3J = 3.5$ Hz, $-\text{N-CH-CH-CH-}$), 8.23, 8.15 (s, 1H, $-\text{N-CH}_2\text{-CO-NH}_2$), 5.51 (s, 2H, $-\text{N-CH}_2\text{-CO-NH}_2$).

1-(2-Amino-2-oxoethyl)-3-carbamoylpyridin-1-ium bromide (2). A solution of nicotinamide (2.0015 g, 16.38 mmol) and 2-bromoacetamide (2.3514 g, 17.04 mmol) was refluxed in acetonitrile for 18 h. After cooling, the white precipitated powder was collected and recrystallized from H_2O /methanol (1 : 3) solution *via* layering with diethyl ether to give the white product **2** with a yield of 3.8360 g (14.75 mmol) or 90%. Column-shaped crystals suitable for single crystal X-ray diffraction were obtained by recrystallization of the product (0.1076 g) from a H_2O (0.5 ml)–2-propanol (10 ml) mixed solvent *via* vapor diffusion of THF. $^1\text{H-NMR}$ (300 MHz, d^6 -DMSO, ppm): 9.41 (s, 1H, $-\text{N-CH-CCO-}$),

9.08–9.06 (d, 1H, $^3J = 5.8$ Hz, $-\text{N-CH-CH-}$), 9.00–8.97 (d, 1H, $^3J = 8.1$ Hz, $-\text{CH-CH-C-CO-}$), 8.55, 7.73 (s, 1H, N-CH-C-CO-NH_2), 8.31–8.26 (t, 1H, $^3J = 7.12$ Hz, $-\text{N-CH-CH-CH-}$), 8.15, 8.05 (s, 1H, $-\text{N-CH}_2\text{-CO-NH}_2$), 5.47 (s, 2H, $-\text{N-CH}_2\text{-CO-NH}_2$).

1-(2-Amino-2-oxoethyl)-3-carbamoylpyridin-1-ium tetrafluoroborate (3). A solution of compound **1** (1.0057 g, 4.66 mmol) in D.I. water (25 ml) was added to a 25 ml $\text{H}_2\text{O}/\text{MeOH}$ solution of AgBF_4 (0.9443 g, 4.85 mmol). The resultant solution was filtered, and the product was collected with a yield of 0.7600 g (2.85 mmol) or 61%. Needle-shaped crystals suitable for single crystal X-ray diffraction were obtained by recrystallization of the product (0.1024 g) from a H_2O (1 ml)–MeOH (30 ml) solution *via* vapor diffusion of diethyl ether. $^1\text{H-NMR}$ (300 MHz, d^6 -DMSO, ppm): 9.39 (s, 1H, $-\text{N-CH-CCO-}$), 9.07–9.05 (d, 1H, $^3J = 5.1$ Hz, $-\text{N-CH-CH-}$), 8.98–8.95 (d, 1H, $^3J = 8.1$ Hz, $-\text{CH-CH-C-CO-}$), 8.53, 7.71 (s, 1H, N-CH-C-CO-NH_2), 8.29–8.25 (t, 1H, $^3J = 6.9$ Hz, $-\text{N-CH-CH-CH-}$), 8.13, 8.03 (s, 1H, $-\text{N-CH}_2\text{-CO-NH}_2$), 5.45 (s, 2H, $-\text{N-CH}_2\text{-CO-NH}_2$).

1-(2-Amino-2-oxoethyl)-3-carbamoylpyridin-1-ium nitrate (4). A solution of compound **1** (1.0064 g, 4.67 mmol) in D.I. water (25 ml) was added to a 25 ml $\text{H}_2\text{O}/\text{MeOH}$ solution of AgNO_3 (0.8299 g, 4.89 mmol). The resultant solution was filtered, and the product was collected with a yield of 0.7287 g (3.01 mmol) or 64%. Plate-shaped crystals suitable for single crystal X-ray diffraction were obtained by recrystallization of the product (0.1043 g) from a H_2O (1 ml)–MeOH (30 ml) solution *via* vapor diffusion of diethyl ether. $^1\text{H-NMR}$ (300 MHz, d^6 -DMSO, ppm): 9.39 (s, 1H, $-\text{N-CH-CCO-}$), 9.08–9.06 (d, 1H, $^3J = 6.1$ Hz, $-\text{N-CH-CH-}$), 8.98–8.96 (d, 1H, $^3J = 8.2$ Hz, $-\text{CH-CH-C-CO-}$), 8.54, 7.71 (s, 1H, N-CH-C-CO-NH_2), 8.30–8.25 (t, 1H, $^3J = 7.1$ Hz, $-\text{N-CH-CH-CH-}$), 8.14, 8.04 (s, 1H, $-\text{N-CH}_2\text{-CO-NH}_2$), 5.46 (s, 2H, $-\text{N-CH}_2\text{-CO-NH}_2$).

1-(2-Amino-2-oxoethyl)-3-carbamoylpyridin-1-ium trifluoromethanesulfonate (5). A solution of compound **1** (1.0005 g, 4.63 mmol) in D.I. water (25 ml) was added to a 25 ml $\text{H}_2\text{O}/\text{MeOH}$ solution of AgOTf (1.2296 g, 4.79 mmol). The resultant solution was filtered, and the product was collected with a yield of 0.8717 g (2.65 mmol) or 57%. Column-shaped crystals suitable for single crystal X-ray diffraction were obtained by recrystallization of the product (0.1024 g) from a MeOH (15 ml) solution *via* vapor diffusion of diethyl ether. $^1\text{H-NMR}$ (300 MHz, d^6 -DMSO, ppm): 9.40 (s, 1H, $-\text{N-CH-CCO-}$), 9.08–9.06 (d, 1H, $^3J = 6.1$ Hz, $-\text{N-CH-CH-}$), 9.00–8.97 (d, 1H, $^3J = 8.1$ Hz, $-\text{CH-CH-C-CO-}$), 8.54, 7.72 (s, 1H, N-CH-C-CO-NH_2), 8.31–8.26 (t, 1H, $^3J = 7.14$ Hz, $-\text{N-CH-CH-CH-}$), 8.14, 8.04 (s, 1H, $-\text{N-CH}_2\text{-CO-NH}_2$), 5.47 (s, 2H, $-\text{N-CH}_2\text{-CO-NH}_2$).

1-(2-Amino-2-oxoethyl)-3-carbamoylpyridin-1-ium hexafluorophosphate (6). A solution of compound **1** (1.0042 g, 4.66 mmol) in D.I. water (25 ml) was added to a 25 ml aqueous solution of NH_4PF_6 (0.7895 g, 4.84 mmol). The resultant solution was filtered, and the product was collected with a yield of 1.4679 g (4.52 mmol) or 83%. Column-shaped crystals suitable for single crystal X-ray diffraction were obtained by recrystallization of the product (0.1011 g) from a H_2O (9 ml)–DMF (1 ml)

mixed solution *via* vapor diffusion of THF. $^1\text{H-NMR}$ (300 MHz, $\text{d}^6\text{-DMSO}$, ppm): 9.40 (s, 1H, $-\text{N-CH-CCO-}$), 9.08–9.06 (d, 1H, $^3J = 5.8$ Hz, $-\text{N-CH-CH-}$), 9.00–8.97 (d, 1H, $^3J = 7.7$ Hz, $-\text{CH-CH-C-CO-}$), 8.56, 7.73 (s, 1H, N-CH-C-CO-NH_2), 8.30–8.26 (t, 1H, $^3J = 7.1$ Hz, $-\text{N-CH-CH-CH-}$), 8.15, 8.05 (s, 1H, $-\text{N-CH}_2\text{-CO-NH}_2$), 5.46 (s, 2H, $-\text{N-CH}_2\text{-CO-NH}_2$).

1-(2-Amino-2-oxoethyl)-3-carbamoylpyridin-1-ium tetraphenylborate (7). A solution of compound **1** (1.0037 g, 4.67 mmol) in D.I. water (25 ml) was added to a 25 ml aqueous solution of NaBPh_4 (1.6577 g, 4.84 mmol). The resultant solution was filtered, and the product was collected with a yield of 1.9977 g (4.00 mmol) or 86%. Plate-shaped crystals suitable for single crystal X-ray diffraction were obtained by recrystallization of the product (0.1051 g) from a THF (15 ml) solution *via* layering of *n*-hexane. $^1\text{H-NMR}$ (300 MHz, $\text{d}^6\text{-DMSO}$, ppm): 9.41 (s, 1H, $-\text{N-CH-CCO-}$), 9.03–9.01 (d, 1H, $^3J = 5.94$ Hz, $-\text{N-CH-CH-}$), 8.98–8.96 (d, 1H, $^3J = 8.1$ Hz, $-\text{CH-CH-C-CO-}$), 8.55, 7.73 (s, 1H, N-CH-C-CO-NH_2), 8.26–8.21 (t, 1H, $^3J = 7.1$ Hz, $-\text{N-CH-CH-CH-}$), 8.16, 8.04 (s, 1H, $-\text{N-CH}_2\text{-CO-NH}_2$), 7.20 (t, 8H, $^3J = 6.8$ Hz, $-\text{B-CH-CH-CH-}$), 6.96–6.91 (t, 8H, $^3J = 7.2$ Hz, $-\text{B-CH-CH-CH-}$), 6.82–6.77 (t, 4H, $^3J = 6.8$ Hz, $-\text{B-CH-CH-CH-}$), 5.45 (s, 2H, $-\text{N-CH}_2\text{-CO-NH}_2$).

X-Ray crystallographic analyses and computation methods

Single-crystal X-ray diffraction data were collected with Mo-K α radiation ($\lambda = 0.71073$ Å) in Φ and ω scan modes using a Bruker APEX-II diffractometer equipped with a CCD array detector with a graphite monochromator. All structures were solved by the direct method and refined (based on F^2 using all independent data) using full-matrix least-squares methods (Bruker SHELXTL 97). In salt **5**, several atoms including one C, three O

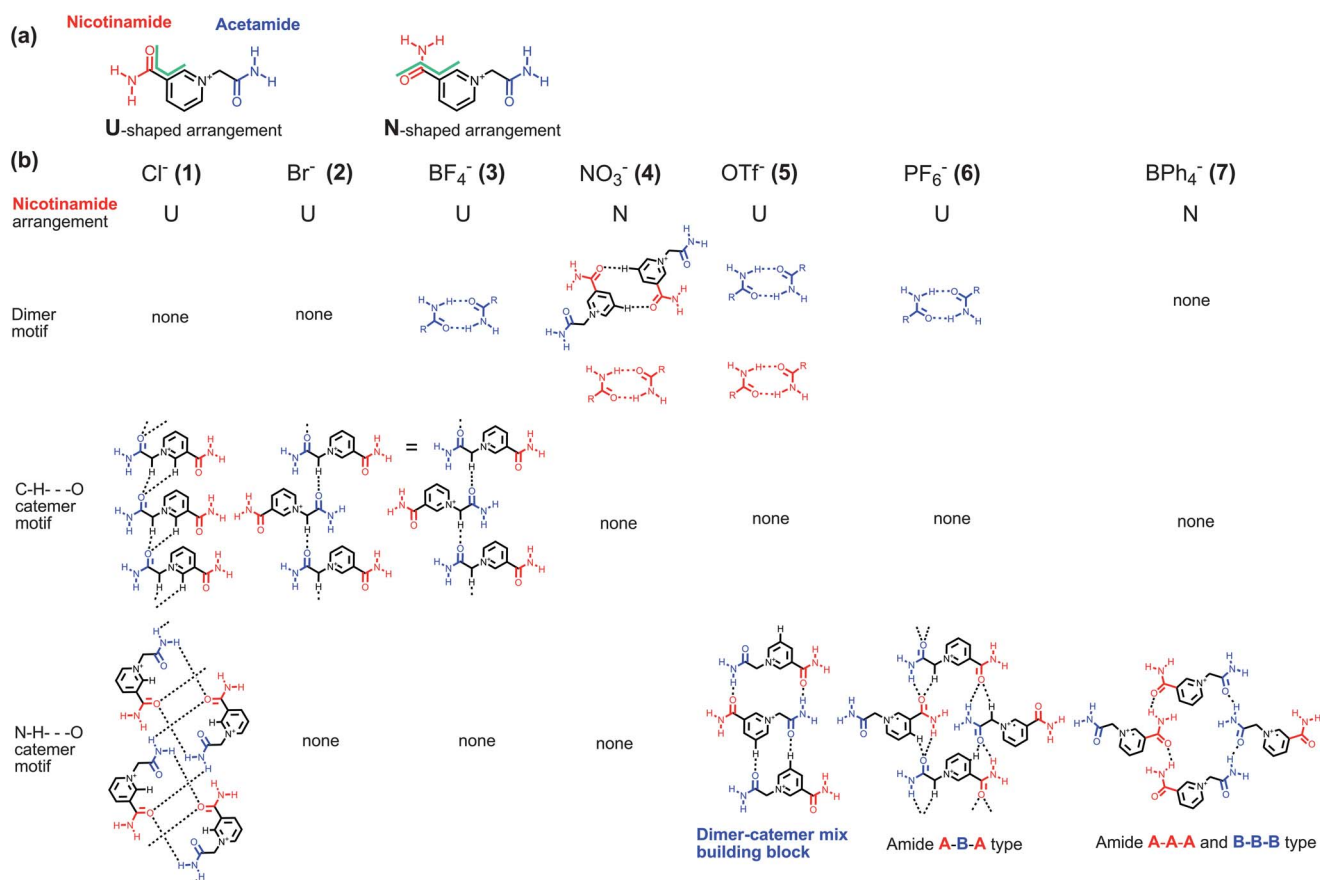
and three F atoms were disordered with two independent orientations having occupancies of 0.73 and 0.27. The non-hydrogen atoms were refined with anisotropic thermal parameters. For the H-atoms, a riding model was employed, except that of salt **7**, in which all the atoms were refined with anisotropic thermal parameters. The details of the crystal parameters, data collection and structure refinements are summarized in Table 1.

Results and discussion

For the convenience of their description and discussion, all of the types of hydrogen bonding motifs adopted in salts **1** to **7** are depicted in Scheme 2. All of the cationic moieties of salts **1** to **7**, 1-(2-amino-2-oxoethyl)-3-carbamoylpyridin-1-ium, exhibit L-shaped structures (Fig. 1(a)). Due to steric hindrance, the acetamide planes are not coplanar with the pyridinium planes, and they adopt torsional angles of $61\text{--}120^\circ$ (θ_1). Notably, the nicotinamide groups of salts **1**, **2**, **3**, **5** and **6** adopt a U-shaped arrangement, and the θ_2 twist angles are less than 38° (Fig. 1(b) and (d)). However, the NO_3^- (**4**) and BPh_4^- (**7**) salts adopt an N-shaped conformation with torsional angles of 155° and 157° , respectively (Fig. 1(c)). In the crystal structure of the Cl^- salt (**1**), there is a twist angle of 38° (θ_2) between the amide plane of the nicotinamide moiety and the pyridinium ring. Two L-shaped cations are bonded to each other *via* $\text{N1-H1A}\cdots\text{O2\#1}$ (Fig. 2(a)) to form a centrosymmetric dimer. Meanwhile, the dimers stack to form a tubular structure involving two types of hydrogen bonding catemers. One is a $\text{C-H}\cdots\text{O}$ catemer which is formed by two $\text{C-H}\cdots\text{O}=\text{C}$ hydrogen bonds ($\text{C3-H3}\cdots\text{O1\#2}$ and $\text{C2-H2A}\cdots\text{O1\#2}$, red and blue dashed lines respectively in Fig. 2(b)) with the carbonyl O atom serving as a bifurcate acceptor. The other is a $\text{N-H}\cdots\text{O}=\text{C}$ hydrogen bonded catemer which is formed by $\text{N1-H1A}\cdots\text{O2\#1}$ and

Table 1 Crystal data and structure refinement for salts **1** to **7**

	1	2	3	4	5	6	7
Empirical formula	$\text{C}_8\text{H}_{10}\text{ClN}_3\text{O}_2$	$\text{C}_8\text{H}_{10}\text{BrN}_3\text{O}_2$	$\text{C}_8\text{H}_{10}\text{BF}_4\text{N}_3\text{O}_2$	$\text{C}_8\text{H}_{10}\text{N}_4\text{O}_5$	$\text{C}_9\text{H}_{10}\text{F}_3\text{N}_3\text{O}_5\text{S}$	$\text{C}_8\text{H}_{10}\text{F}_6\text{N}_3\text{O}_2\text{P}$	$\text{C}_{32}\text{H}_{30}\text{BN}_3\text{O}_2$
Formula weight	215.64	260.10	267.00	242.20	329.26	325.16	499.40
Crystal system	Monoclinic	Monoclinic	Monoclinic	Triclinic	Triclinic	Orthorhombic	Orthorhombic
T/K	100	100	100	296	100	100	100
Space group	$P1$	$P2_1/n$	$P2_1/c$	$P1$	$P1$	$Pbca$	$Pca2_1$
$a/\text{\AA}$	5.3951(4)	10.3283(8)	11.5624(4)	5.4520(3)	8.4003(2)	13.2470(10)	9.7596(3)
$b/\text{\AA}$	8.1557(7)	8.1976(7)	8.3426(4)	6.1264(3)	8.9153(2)	11.2054(10)	15.6860(5)
$c/\text{\AA}$	11.4412(9)	12.3290(9)	12.2163(5)	15.5624(8)	10.3151(3)	15.5055(14)	16.8530(5)
α/deg	80.447(2)	90	90.00	99.478	101.5700(10)	90	90
β/deg	84.791(2)	114.243(3)	116.412	92.657(3)	103.4520(10)	90	90
γ/deg	72.016	90	90.00	99.407(3)	111.6400(10)	90	90
$V/\text{\AA}^3$	471.77(7)	951.81(13)	1055.39(8)	504.38(5)	662.40(3)	2301.6(3)	2580.01(14)
Z	2	4	4	2	2	8	4
$D_{\text{calc}}/\text{g cm}^{-3}$	1.518	1.815	1.680	1.595	1.651	1.877	1.286
μ/mm^{-1}	0.382	4.296	0.165	0.134	0.307	0.327	0.080
θ/deg	1.81 to 26.53	3.08 to 26.36	1.97 to 26.38	1.33 to 26.45	2.14 to 26.51	2.72 to 26.40	1.30 to 26.40
Range h	–6 to 6	–8 to 12	–14 to 14	–6 to 6	–10 to 10	–16 to 16	–10 to 12
Range k	–10 to 10	–10 to 10	–10 to 10	–7 to 7	–8 to 11	–13 to 14	–19 to 19
Range l	–13 to 14	–15 to 15	–14 to 15	–19 to 19	–12 to 12	–19 to 19	–20 to 21
Reflns collected	7994	7935	8738	8320	10 291	17 454	20 147
Unique reflns	1933	1937	2137	2060	2702	2356	5121
Data/restraints/parameters	1933/0/127	1937/0/127	2137/0/163	2060/0/154	2702/0/190	2356/0/181	5121/1/343
$R_1, wR_2 [I > 2\sigma(I)]$	0.0258, 0.0679	0.0168, 0.0416	0.0309, 0.0783	0.0338, 0.1044	0.0336, 0.0358	0.0290, 0.0714	0.0343, 0.0862
R_1, wR_2 (all data)	0.0268, 0.0687	0.0182, 0.0420	0.0332, 0.0805	0.0382, 0.1196	0.0832, 0.0847	0.0383, 0.0775	0.0425, 0.1102
GOF	1.068	1.049	1.075	1.930	1.056	1.053	1.153
CCDC number	838304	838305	838306	838307	838308	838309	838310



Scheme 2 (a) There are two conformations formed by nicotinamide groups. One conformation is the U-shaped conformation, and the other is the N-shaped conformation (green lines). (b) The hydrogen bonding dimer and catemer motifs of the seven salts in this study.

N1#3–H1B#3...O2 (green dashed lines in Fig. 2(b)). Notably, this N–H...O=C catemer is formed by carbonyl O atoms of nicotinamide (bifurcate acceptors) and NH₂ groups of acetamide alternatively (Fig. 2(b) and Scheme 2(b)). The Cl⁻ anions are located between the cationic tubular structures, and they form two N–H...Cl⁻ and two C–H...Cl⁻ hydrogen bonds (Fig. 2(c)). In the crystal structure of the Br⁻ salt (2), the amide

plane in the nicotinamide moiety is also not coplanar with the pyridinium ring and has a twist angle of 28° (θ_2). However, unlike the tubular structures in 1, the cationic moieties of 2 stack in an interdigitated fashion to form a two dimensional brick packing structure *via* a mixed C–H...O/N–H...O type of catemer (C2#2–H2A#2...O1 and N2#2–H1B#2...O1 bonds in Fig. 3(a)).

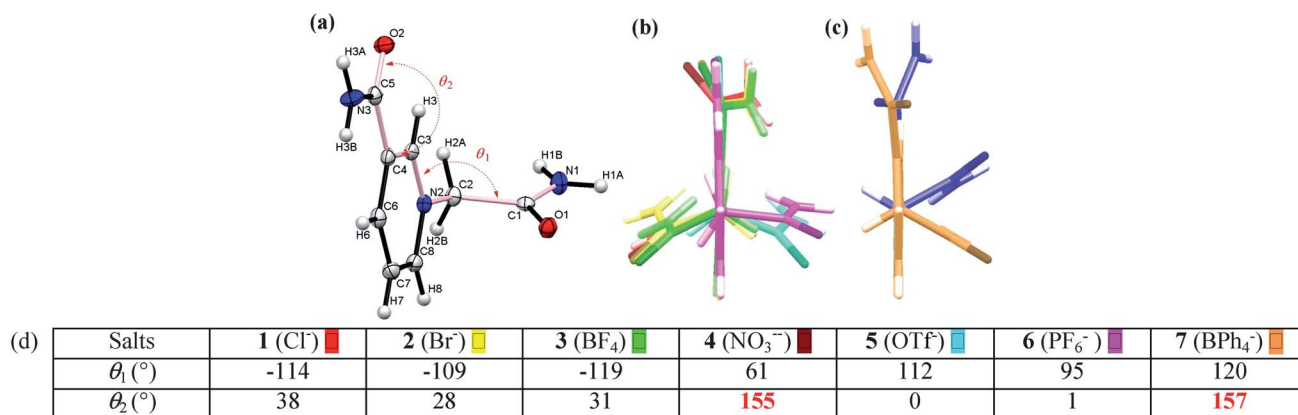


Fig. 1 (a) ORTEP drawing of the 1-(2-amino-2-oxoethyl)-3-carbamoylpyridin-1-ium cation moiety of PF₆⁻ salt 6 with atomic numbering and the definitions of the two torsional angles θ_1 and θ_2 . (b) and (c) Superposition of the cations with side views of the pyridinium rings and a view along the C6...N2–C2 direction. (b) 1 (Cl⁻, red), 2 (Br⁻, yellow), 3 (BF₄⁻, green), 5 (OTf⁻, pale blue) and 6 (PF₆⁻, pink). (c) 4 (NO₃⁻, purple) and 7 (BPh₄⁻, orange). The nicotinamide groups of both salts adopt an N-shaped conformation. (d) The torsion angle of θ_1 (C3–N2–C2–C1) and θ_2 (C3–C4–C5–O2) of salts 1–7.

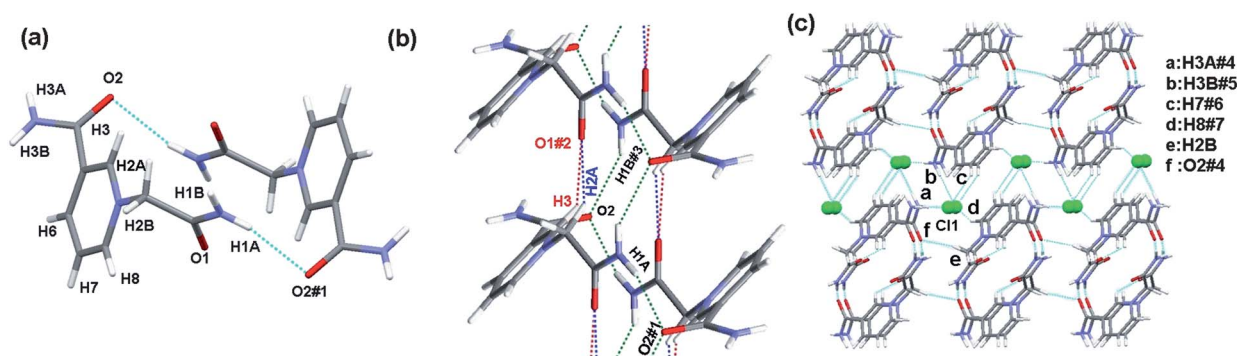


Fig. 2 The hydrogen bonding motif and packing of the Cl^- salt (**1**). (a) The dimer building block (Symm. Op. #1 = $1 - x, 1 - y, 2 - z$), (b) double catemer motifs (Symm. Op. #2 = $-1 + x, y, z$; #3 = $-x, 1 - y, 2 - z$) and (c) the arrangement of the cationic tubular structures that surround the Cl^- anions in the packing (Symm. Op. #4 = $1 + x, -1 + y, z$; #5 = $-x, 1 - y, 1 - z$; #6 = $1 - x, 1 - y, 1 - z$; #7 = $-1 + x, y, z$). The detailed hydrogen bonding data are listed in Table 2.

Table 2 Hydrogen bonding details of salt **1**

D-H...A	D-H/Å	H...A/Å	D...A/Å	$\angle\text{D-H...A}/^\circ$
N1-H1A...O2#1	0.88	2.16	3.03	166
C3-H3...O1#2	0.95	2.34	3.06	132
C2-H2A...O1#2	0.99	2.44	3.27	141
N1#3-H1B#3...O2	0.88	2.26	3.26	138
C2-H2B...O2#4	0.99	2.49	3.37	148
C7#6-H7#6...Cl1	0.95	2.84	3.64	143
C8#7-H8#7...Cl1	0.95	2.52	3.38	151
N3#4-H3A#4...Cl1	0.88	2.29	3.17	172
N3#5-H3B#5...Cl1	0.88	2.36	3.21	162

Table 3 Hydrogen bonding details of salt **2**

D-H...A	D-H/Å	H...A/Å	D...A/Å	$\angle\text{D-H...A}/^\circ$
C2-H2A...O1#1	0.99	2.36	3.31	161
N1#2-H1B#2...O2#3	0.88	2.28	3.06	147
C2#4-H2B#4...Br1	0.99	2.86	3.67	140
N1#5-H1A#5...Br1	0.88	2.70	3.51	153
N3#6-H3A#6...Br1	0.88	2.78	3.59	153
C7#7-H7#7...Br1	0.95	3.03	3.82	142
C8#8-H8#8...Br1	0.95	3.03	3.68	127
N3#8-H3B#8...Br1	0.88	5/20	3.35	164

The Br^- anions are located between two pyridinium rings (Fig. 3(b)) and form six hydrogen bonds, including two $\text{C-H}\cdots\text{O}=\text{C}$, one $\text{C}_\alpha\text{-H}\cdots\text{O}=\text{C}$ and three $\text{N-H}\cdots\text{O}=\text{C}$ hydrogen bonds, which are shown in Fig. 3(c). A comparison of the structures of salts **1** and **2** indicates that the hydrogen bonding catemers formed by the acetamide groups are *syn*-orientated in **1** and *anti*-orientated in **2**. This difference is likely a result of the size of the anions because the distance between two neighboring acetamide groups on the same side of the structure is 8.198 Å, which would allow the larger Br^- anion to fit in a condensed packing arrangement. It is worth noting that the hydrogen bonding catemers in **1** and **2** consist of conventional $\text{N-H}\cdots\text{O}=\text{C}$ and nonconventional $\text{C-H}\cdots\text{O}=\text{C}$ hydrogen bonds, which

indicates that the latter could serve as an alternative to the N-H donor in the crystal packing. In the crystal structure of the BF_4^- salt (**3**), a two-dimensional brick packing structure is formed. The amide plane of the nicotinamide moiety is not coplanar with the pyridinium ring and has a twist angle of 31° (θ_2). Fig. 4(a) depicts the two-dimensional brick packing structure of **3** which contains one more $\text{N-H}\cdots\text{O}=\text{C}$ hydrogen bonded dimer motif (N1#2-H1A#2...O1#1) when compared to the brick structure of the Br^- salt. Like the Br^- anions in **2**, the BF_4^- anions of **3** are located between two pyridinium rings and form six hydrogen bonds, including two $\text{C}_{\text{ring}}\text{-H}\cdots\text{F}$, one $\text{C}_\alpha\text{-H}\cdots\text{F}$ and three $\text{N-H}\cdots\text{F}$ hydrogen bonds, which are shown in Fig. 4(c). Fig. 5 depicts the ribbon building block of the NO_3^- salt (**4**). The amide

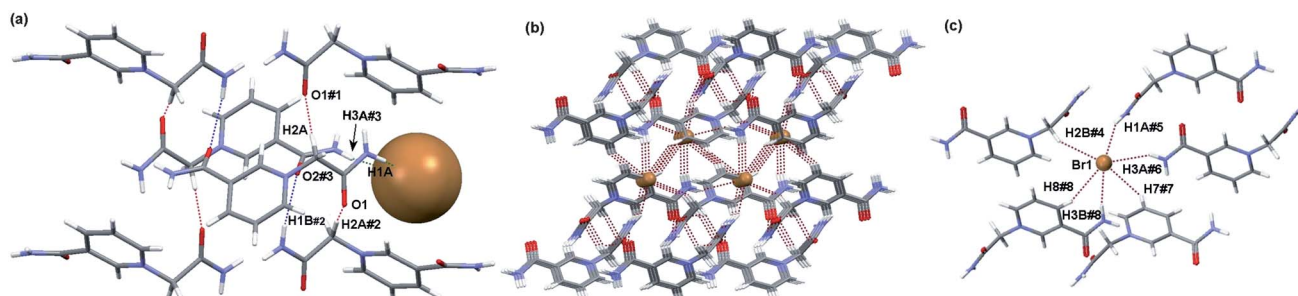


Fig. 3 The hydrogen bonding motif and packing of the Br^- salt (**2**). (a) Catemer motifs (Symm. Op. #1 = $1 - x, 1 - y, 2 - z$; #2 = $1/2 - x, 1/2 + y, 3/2 - z$; #3 = $1/2 - x, 1/2 + y, 3/2 - z, -1/2 + x, 3/2 - y, -1/2 + z$). (b and c) The arrangement of the cationic brick structure with the intercalated Br^- anions in the packing (Symm. Op. #4 = $1/2 - x, 1/2 + y, 3/2 - z$; #5 = $1/2 + x, 3/2 - y, 1/2 + z$; #6 = $3/2 - x, 1/2 + y, 5/2 - z$; #7 = $1 + x, y, z$; #8 = $1/2 + x, 3/2 - y, -1/2 + z$). The detailed hydrogen bonding data are listed in Table 3.

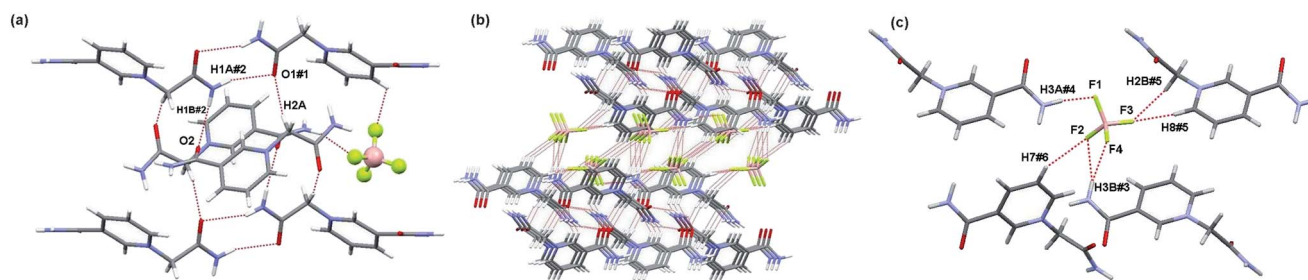


Fig. 4 The hydrogen bonding motif and packing of the BF_4^- salt (**3**). (a) The dimer building block (Symm. Op. #1 = $2 - x, 1/2 + y, 3/2 - z$; #2 = $x, 1/2 - y, -1/2 + z$), (b) catemer motifs and (c) the arrangement of the cationic brick structure with the intercalated BF_4^- anions in the packing (Symm. Op. #3 = $x, 1 + y, z$; #4 = $1 - x, 1 - y, -z$; #5 = $1 - x, 1 - y, 1 - z$; #6 = $x, 1/2 - y, -1/2 + z$). The detailed hydrogen bonding data are listed in Table 4.

Table 4 Hydrogen bonding details of salt **3**

D–H...A	D–H/Å	H...A/Å	D...A/Å	$\angle\text{D–H...A}/^\circ$
C2–H2A...O1#1	0.99	2.61	3.60	172
N1#2–H1B#2...O2	0.88	2.21	2.98	146
N1#2–H1A#2...O1#1	0.88	2.26	3.06	151
N3#3–H3B#3...F2	0.88	2.60	3.42	155
N3#3–H3B#3...F4	0.88	2.16	2.94	148
N3#4–H3A#4...F1	0.88	2.13	2.95	155
C2#5–H2B#5...F3	0.99	2.34	3.07	131
C8#5–H8#5...F3	0.95	2.56	3.28	133
C7#6–H7#6...F2	0.95	2.41	3.18	138

Table 5 Hydrogen bonding details of salt **4**

D–H...A	D–H/Å	H...A/Å	D...A/Å	$\angle\text{D–H...A}/^\circ$
C8–H8...O4	0.93	2.34	3.14	143
C3#3–H3#3...O3	0.93	2.18	3.08	165
C7#1–H7#1...O2	0.93	2.65	3.27	124
N3#2–H3A#2...O2	0.86	2.10	2.95	168
C2#6–H2A#6...O5	0.97	2.50	3.43	160
N1#4–H1A#4...O5	0.97	2.15	2.98	163
N1#5–H1B#5...O3	0.86	2.26	2.95	138
N1#5–H1B#5...O5	0.86	2.40	3.25	167
N3#3–H3B#3...O4	0.86	2.19	2.99	155

group of the nicotinamide moiety adopts a N-shaped conformation, which is the opposite arrangement of the U-shaped conformation (Scheme 2(a)); in other words, the directions of the C=O and NH_2 groups are exchanged, and the C=O group adopts a large twist angle of 155° relative to the plane of the pyridinium ring. The C=O groups serve as bifurcate hydrogen bonding acceptors and form alternative C–H...O (C7#1–H7#1...O2) and N–H...O (N3#2–H3A#2...O2) hydrogen bonding dimer motifs. The continuous dimer motifs result in a ribbon building block (Fig. 5(a)).

The NO_3^- anions are located between the ribbons and form seven hydrogen bonds, including two $\text{C}_{\text{ring}}\text{–H...O}=\text{C}$ (C8–

H8...O4, and C3#3–H3#3...O3), one $\text{C}_\alpha\text{–H...O}=\text{C}$ (C2#6–H2B#6...O5) and four N–H...O=C hydrogen bonds (N3#3–H3B#3...O4, N1#5–H1B#5...O3, N1#5–H1B#5...O5 and N1#3–H1B#3...O5), which are shown in Fig. 5(b). In the crystal structure of the OTf^- salt (**5**), the amide plane of the nicotinamide moiety is coplanar with the pyridinium ring ($\theta_2 = 0$). A linear tape building block is formed by two alternative dimer motifs; one such building block is formed *via* a N–H...O type (N1–H1B...O2#1) bonding interaction, and the other is formed *via* a C–H...O type (C–H7...O1#2) interaction as depicted in Fig. 6(a). The acetamide group of salt **5** possesses a twist angle of 112° relative to the pyridinium ring and bonds to the other amide groups of the cations in the neighboring tape with bond distances

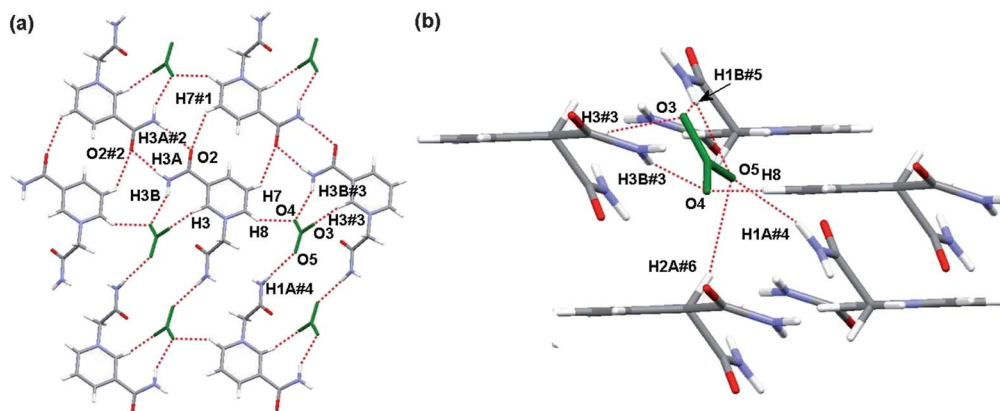


Fig. 5 The hydrogen bonding motif and packing of the NO_3^- salt (**4**) (Symm. Op. #1 = $1 - x, -y, 1 - z$; #2 = $2 - x, -1 - y, 1 - z$; #3 = $-1 + x, 1 + y, z$; #4 = $2 - x, 1 - y, 2 - z$; #5 = $1 - x, 1 - y, 2 - z$; #6 = $x, 1 + y, z$). (a) The ribbon building block and (b) the arrangement of the cationic ribbon structure and the intercalated NO_3^- anions in the packing. The detailed hydrogen bonding data are listed in Table 5.

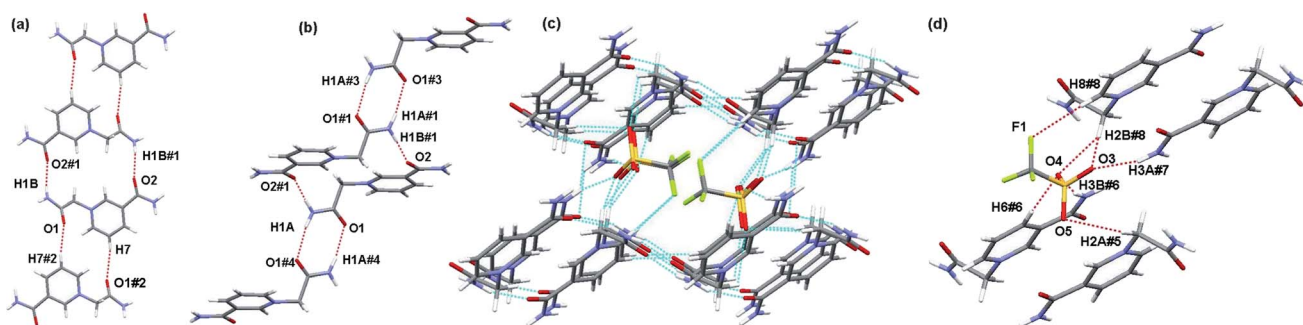


Fig. 6 The hydrogen bonding motif and packing of the OTF^- salt (**5**). (a) The tape building block formed by the dimer/catemer mixed motif (Symm. Op. #1 = $1 - x, 2 - y, 1 - z$; #2 = $1 - x, -1 - y, -z$) and (b) the dimer motif serves as an inter-tape linkage (Symm. Op. #3 = $1 - x, 1 - y, 1 - z$; #4 = $x, y, -1 + z$). (c and d) show the arrangement of the cationic tape structure and the intercalated OTF^- anions in the packing (Symm. Op. #5 = $x, y, 1 + z$; #6 = $1 - x, 2 - y, 1 - z$; #7 = $-1 + x, -1 + y, 1 + z$; #8 = $-x, 1 - y, 1 - z$). The detailed hydrogen bonding data are listed in Table 6.

Table 6 Hydrogen bonding details of salt **5**

D–H...A	D–H/Å	H...A/Å	D...A/Å	$\angle\text{D–H...A}/^\circ$
N1–H1B#1...O2	0.88	2.03	2.88	162
C7–H7...O1#2	0.95	2.38	3.31	165
N1#1–H1A#1...O1#3	0.88	2.06	2.92	167
C2#5–H2A#5...O5	0.99	2.70	3.41	137
C6#6–H6#6...O4	0.95	2.34	3.27	166
N3#7–H3A#7...O3	0.88	2.18	2.96	147
C8#8–H8#8...F1	0.95	2.62	3.57	174
C2#8–H2B#8...O3	0.99	2.65	3.47	141
C2#8–H2B#8...O4	0.99	2.41	3.28	146
N3#6–H3B#6...O4	0.88	2.08	2.94	164

of 2.06 Å (N1#1–H1A#1...O1#3, Fig. 6(b)). This typical amide dimer motif serves as a linkage between the tapes to form a two-dimensional grid structure. The OTF^- anions are located within the cavities of the grid (Fig. 6(c)) and form two $\text{C}_{\text{ring}}\text{--H}\cdots\text{O}$ hydrogen bonds (C6#6–H6#6...O4 and C8#8–H8#8...F1), three $\text{C}_\alpha\text{--H}\cdots\text{O}$ hydrogen bonds (C2#5–H2A#5...O5, C2#8–H2B#8...O3 and C2#8–H2B#8...O4) and two $\text{N--H}\cdots\text{O}$ hydrogen bonds (N3#7–H3A#7...O3 and N3#6–H3B#6...O4),

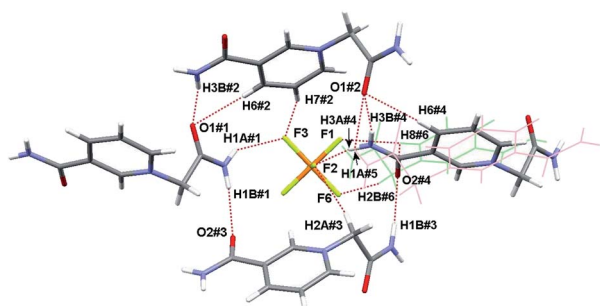


Fig. 7 The hydrogen bonding motif and packing of the PF_6^- salt (**6**). The sheet structure is formed by alternating nicotinamide and acetamide moieties *via* $\text{C--H}\cdots\text{O}/\text{N--H}\cdots\text{O}$ hydrogen bonding catemers. The *anti*-oriented catemer arrangement with the intercalated PF_6^- anions in the packing (Symm. Op. #1 = $-x, 1/2 + y, 1/2 - z$; #2 = $1/2 - x, 2 - y, -1/2 + z$; #3 = $1/2 - x, 1/2 + y, z$; #4 = $1 - x, 1/2 + y, 1/2 - z$; #5 = $1/2 + x, 1 + y, 1/2 - z$; #6 = $1/2 + x, y, 1/2 - z$). The detailed hydrogen bonding data are listed in Table 7.

which are shown in Fig. 6(d). In the crystal structure of the PF_6^- salt (**6**), the amide plane of the nicotinamide moiety is nearly coplanar with the pyridinium ring ($\theta_2 = 0$). Fig. 7 depicts the two-dimensional sheet packing structure of the PF_6^- salt **6**. Notably, the hydrogen bonding catemers *via* pure amide groups are formed by the alteration of nicotinamide and acetamide moieties *via* two sets of hydrogen bonding interactions. The first set of interactions is the $\text{N--H}\cdots\text{O}=\text{C}$ (N3#2–H3B#2...O1#1) and $\text{C--H}\cdots\text{O}=\text{C}$ (C6#2–H6#2...O1#1) hydrogen bonding interactions, and the second set is the $\text{N--H}\cdots\text{O}=\text{C}$ (N1#1–H1B#1...O2#3) hydrogen bonding interaction. The PF_6^- anions, like those in the Br^- and BF_4^- salts, are located between two pyridinium rings and form seven hydrogen bonds, including two $\text{C--H}\cdots\text{O}=\text{C}$ (C7#2–H7#2...F3 and C8#6–H8#6...F1), two $\text{C}_\alpha\text{--H}\cdots\text{O}=\text{C}$ (C2#3–H2A#3...F2 and C2#6–H2B#6...F6) and two $\text{N--H}\cdots\text{O}=\text{C}$ hydrogen bonds (N1#1–H1A#1...F3 and N3#4–H3A#4...F2), which are shown in Fig. 7. In the crystal structure of the BPh_4^- salt (**7**), as in the NO_3^- salt (**4**), the amide plane of the nicotinamide moiety adopts a large twist angle relative to the pyridinium ring ($\theta_2 = 157^\circ$). Fig. 8(a) depicts the two-dimensional sheet packing structure of the BPh_4^- salt **7**. However, the types of hydrogen bonding amide hydrogen bonding catemers in salt **7** differ from those in salt **6**. Two hydrogen bonding catemers in salt **7** are formed by pure nicotinamide or acetamide groups with $\text{N--H}\cdots\text{O}=\text{C}$ hydrogen bonding respectively (N1#2–H1B#2...O1 and N3–H3B...O2#1 Fig. 8(a)). The amide plane of the nicotinamide moiety adopts an opposite conformation like that observed in the NO_3^- salt **4** (Fig. 5(a) and Scheme 1). The

Table 7 Hydrogen bonding details of salt **6**

D–H...A	D–H/Å	H...A/Å	D...A/Å	$\angle\text{D–H...A}/^\circ$
N3#2–H3B#2...O1#1	0.88	2.04	2.90	163
C6#2–H6#2...O1#1	0.95	2.38	3.30	162
N1#1–H1B#1...O2#3	0.88	2.10	2.94	157
C7#2–H7#2...F3	0.95	2.47	3.38	160
C8#6–H8#6...F1	0.95	2.49	3.38	156
C2#3–H2A#3...F2	0.99	2.51	3.48	165
C2#6–H2B#6...F6	0.99	2.46	3.43	167
N1#1–H1A#1...F3	0.88	2.34	3.10	145
N3#4–H3A#4...F2	0.88	2.16	3.00	160

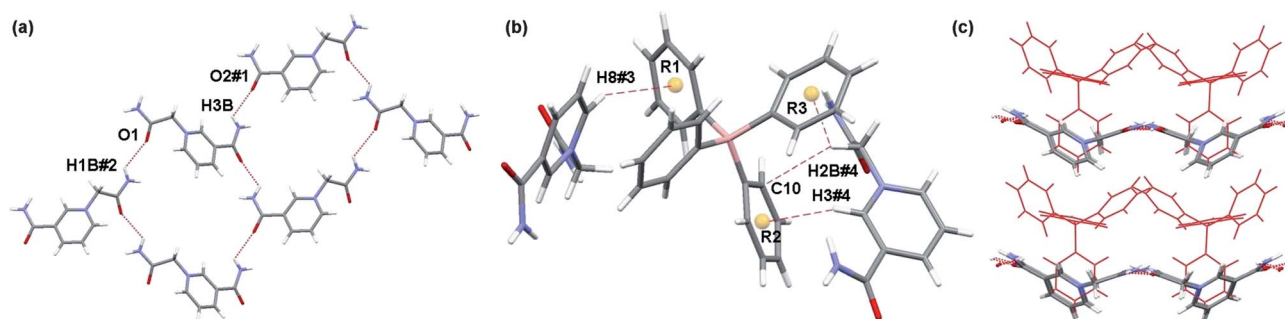


Fig. 8 The hydrogen bonding motifs in the packing structure of the BPh_4^- salt (7). (a) The sheet structure formed by the $\text{N-H}\cdots\text{O}$ hydrogen bonding catemer motif. (b) The formation of the $\text{C-H}\cdots\pi$ interactions by cations and BPh_4^- anions. (c) The BPh_4^- anions are intercalated between the cationic sheet structures (Symm. Op. #1 = $-1/2 + x, 2 - y, z$; #2 = $1/2 + x, 1 - y, z$; #3 = $1 + x, y, -1 + z$; #4 = $1/2 - x, y, -1/2 + z$). The detailed hydrogen bonding data are listed in Table 8.

Table 8 Hydrogen bonding details of salt 7

D-H...A	D-H/Å	H...A/Å	D...A/Å	$\angle\text{D-H}\cdots\text{A}/^\circ$
N1#2-H1B#2...O1	0.90(3)	2.23(3)	2.977(2)	127(2)
N3-H3B...O2#1	0.86(3)	2.35(3)	2.839(2)	128(2)
C8#3-H8#3...R1	0.94(2)	2.51	3.34	147
C3#4-H3#4...R2	0.90(2)	2.71	3.35	128
C2#4-H2B#4...R3	0.95(2)	2.57	3.26	130
C2#4-H2B#4...C10	1.02(2)	2.81(2)	3.394(3)	121(2)

BPh_4^- anions are located between sheets and form four $\text{C-H}\cdots\pi$ hydrogen bonds, including two $\text{C-H}\cdots\pi$ (C8#3-H8#3...R1 and C3#4-H3#4...R2) and two $\text{C}_\alpha\text{-H}\cdots\pi$ (C2#4-H2B#4...R3 and C2#4-H2B#4...C10) hydrogen bonds, which are shown in Fig. 8(b) and (c). The $\text{C-H}\cdots\pi$ hydrogen bonds are similar to those in the pyridinium BPh_4^- salt.³⁸

On the basis of the crystal structures of salts 1 to 7, we drew the following conclusions: (1) The diamide pyridinium salts may aggregate convergently to form tubular structures (Cl^- (1)) or divergently to form a one-dimensional ribbon structure (NO_3^- (4)) or two-dimensional brick (Br^- (2) and BF_4^- (3)), grid (OTf^- (5) and PF_6^- (6)) and sheet structures (BPh_4^- (7)). (2) The hydrogen bonding catemer motifs *via* the amide C=O acceptor are reliable building units for all of the salts with spherical or regular polyhedral anions, Cl^- (1), Br^- (2), BF_4^- (3), PF_6^- (6) and BPh_4^- (7). These motifs include the conventional $\text{N-H}\cdots\text{O}$ type (BPh_4^- (7)), the nonconventional $\text{N-H}\cdots\text{O}$ types (Cl^- (1)) and, the mixed $\text{N-H}\cdots\text{O}/\text{C-H}\cdots\text{O}$ type (OTf^- (5) and PF_6^- (6)), and the interesting pure $\text{C-H}\cdots\text{O}$ types (Cl^- (1), Br^- (2) and BF_4^- (3)). These results clearly demonstrate that the charge-enhanced C-H group is able to bond to carbonyl O atoms and is also robust enough to be an alternative hydrogen bond donor in the construction of $\text{C-H}\cdots\text{O}$ hydrogen bonding catemers. Thus, this finding could also expand the flexibility of the amide group in variable hydrogen bonding catemer motifs. (3) It appears that the size of the anions plays a significant role in the type of hydrogen bonding catemer, because these $\text{N-H}\cdots\text{O}$ types were only observed in the species with relatively larger anions (PF_6^- (6) and BPh_4^- (7)). Additionally, the type of four typical motifs (Scheme 1) is also affected by the size of anion species, thus the *syn*-oriented hydrogen bonding catemers were only observed in the species

with the smallest anion (Cl^-), but they form *anti*-oriented hydrogen bonding catemers in the other four salts. This observation can be explained by the large separation of *anti*-oriented hydrogen bonding catemer that is suitable for large anions. Intriguingly, the cationic moieties of the NO_3^- and BPh_4^- salts adopt the N-shaped conformation. One reason for this phenomenon is the tendency of the NO_3^- salt to achieve the maximum number of hydrogen bonds with the NO_3^- anions, which would overcome the energy lost by adopting the N-shaped conformation. As for the BPh_4^- salts, the conformation may be a result of the size effect simply because the BPh_4^- anion is very large in size. Additionally, BPh_4^- is a very weak hydrogen bond acceptor. Therefore, to be compatible with the anion size, the cationic moieties adopt the N-shaped conformation and form a sheet structure to maximize the space that could be occupied by an anion. Notably, the sheet formed in the BPh_4^- salt is different from the smaller sheet structure observed in the structure containing the PF_6^- anion (Fig. 7) in which the U-shaped structure is adopted.

Conclusions

Here we reported a series of diamide-containing pyridinium salts. The L-shaped cations could aggregate convergently to form a tubular structure or divergently to form a one-dimensional ribbon structure or two-dimensional brick, grid and sheet structures *via* variable hydrogen bonding catemers. Additionally, the size of the anion plays a significant role in determining the types of hydrogen bonding catemer motifs that form. These results not only imply the importance of $\text{C-H}\cdots\text{O}=\text{C}$ hydrogen bonding, which is able to serve as an alternative to the $\text{N-H}\cdots\text{O}=\text{C}$ hydrogen bonding in hydrogen bonding catemer motifs, but also allow us to design better, new supramolecular architectures.

Acknowledgements

The work was supported by the National Science Council of Taiwan, Republic of China (NSC-100-2113-M-017-001) and National Kaohsiung Normal University. We are grateful to the National Center for High-performance Computing for computer time and facilities.

Notes and references

- 1 G. R. Desiraju, *Chem. Commun.*, 2005, 2995–3001.
- 2 G. R. Desiraju, *Acc. Chem. Res.*, 2002, **35**, 565–573.
- 3 S. S. Kuduva, D. C. Craig, A. Nangia and G. R. Desiraju, *J. Am. Chem. Soc.*, 1999, **121**, 1936–1944.
- 4 G. R. Desiraju and T. Steiner, *The Weak Hydrogen Bond in Structural Chemistry and Biology*, Oxford University Press, Oxford, U.K., 1999.
- 5 T. Steiner, *Chem. Commun.*, 1997, 727–734.
- 6 G. R. Desiraju, *Acc. Chem. Res.*, 1996, **29**, 441–449.
- 7 C. R. Kaiser, K. C. Pais, M. V. N. de Souza, J. L. Wardell, S. M. S. V. Wardell and E. R. T. Tiekink, *CrystEngComm*, 2009, **11**, 1133–1140.
- 8 A. Solano-Peralta, J. P. Saucedo-Vázquez, R. Escudero, H. Höpfl, H. El-Mkami, G. M. Smith and M. E. Sosa-Torres, *Dalton Trans.*, 2009, 1668–1674.
- 9 L.-F. Ma, L.-Y. Wang, J.-L. Hu, Y.-Y. Wang, S. R. Batten and J.-G. Wang, *CrystEngComm*, 2009, **11**, 777–783.
- 10 H. Zhou, L. Chen, R. Chen, Z.-H. Peng, Y. Song, Z.-Q. Pan, Q.-M. Huang, X.-L. Hu and Z.-W. Bai, *CrystEngComm*, 2009, **11**, 671–679.
- 11 Y. R. Zhong, M. L. Cao, H. J. Mo and B. H. Ye, *Cryst. Growth Des.*, 2008, **8**, 2282–2290.
- 12 S. Takahashi, T. Jukurogi, T. Katagiri and K. Uneyama, *CrystEngComm*, 2006, **8**, 320–326.
- 13 J. G. Planas, C. Masalles, R. Sillanpää, R. Kivekäs, F. Teixidor and C. Viñas, *CrystEngComm*, 2006, **8**, 75–83.
- 14 A. N. Sokolov, T. Friscic, S. Blais, J. A. Ripmeester and L. R. MacGillivray, *Cryst. Growth Des.*, 2006, **6**, 2427–2428.
- 15 J. W. Steed and J. L. Atwood, *Supramolecular Chemistry*, VCH, New York, 2000.
- 16 C. J. Janiak, *J. Chem. Soc., Dalton Trans.*, 2000, 3885–3896.
- 17 G. A. Jeffrey, *An Introduction to Hydrogen Bonding*, Oxford University Press, Oxford, U.K., 1997.
- 18 D. R. Armstrong, M. G. Davidson and D. Moncrief, *Angew. Chem., Int. Ed. Engl.*, 1995, **34**, 478–481.
- 19 C. Coletti and N. Re, *J. Phys. Chem. A*, 2009, **113**, 1578–1585.
- 20 S. K. Panigrahi, *Amino Acids*, 2008, **34**, 617–633.
- 21 G. Toth, S. G. Bowers, A. P. Truong and G. Probst, *Curr. Pharm. Des.*, 2007, **13**, 3476–3493.
- 22 S. Sarkhel and G. R. Desiraju, *Proteins: Struct., Funct., Genet.*, 2004, **54**, 247–259.
- 23 E. Arbely and I. T. Arkin, *J. Am. Chem. Soc.*, 2004, **126**, 5362–5363.
- 24 K. Manikandan and S. Ramakumar, *Proteins: Struct., Funct., Bioinf.*, 2004, **56**, 768–781.
- 25 S. Aravinda, N. Shamala, A. Bandyopadhyay and P. Balaram, *J. Am. Chem. Soc.*, 2003, **125**, 15065–15075.
- 26 B. K. Ho and P. M. Curmi, *J. Mol. Biol.*, 2002, **317**, 291–308.
- 27 M. C. Wahl and M. Sundaralingam, *Trends Biochem. Sci.*, 1997, **22**, 97–102.
- 28 O. B. Berryman, V. S. Bryantsev, D. P. Stay, D. W. Johnson and B. P. Hay, *J. Am. Chem. Soc.*, 2007, **129**, 48–58.
- 29 Y. Bai, B.-G. Zhang, C.-Y. Duan, D.-B. Dang and Q.-J. Meng, *New J. Chem.*, 2006, **30**, 266–271.
- 30 I. Hisaki, S.-I. Sasaki, K. Hirose and Y. Tobe, *Eur. J. Org. Chem.*, 2007, 607–615.
- 31 K.-J. Chang, D. Moon, M. S. Lah and K.-S. Jeong, *Angew. Chem., Int. Ed.*, 2005, **44**, 7926–7929.
- 32 H. Ihm, S. Yun, H. G. Kim, J. K. Kim and K. S. Kim, *Org. Lett.*, 2002, **4**, 2897.
- 33 A. Bianchi, K. Bowman-James and E. García-España, *Supramolecular Chemistry of Anions*, Wiley-VCH, New York, 1997.
- 34 A.-S. Wilkinson, P. K. Bryant, S. O. Meroueh, M. G. P. Page, S. Mobashery and C. W. Wharton, *Biochemistry*, 2003, **42**, 1950–1957.
- 35 R. E. Melendez and A. D. Hamilton, *Design of Organic Solids: Hydrogen-Bonded Ribbons, Tapes and Sheets as Motifs*, Springer-Verlag, Berlin, 1998.
- 36 K. M. Lee, Y. T. Lee and I. J. B. Lin, *J. Mater. Chem.*, 2003, **13**, 1079–1084.
- 37 C. H. Lee, F. Y. Su, Y. H. Lin, C. H. Chou and K. M. Lee, *CrystEngComm*, 2011, **13**, 2318–2323.
- 38 D. Jin, F. Zhang, Y. Zhang and D.-C. Zhang, *Acta Crystallogr., Sect. E: Struct. Rep. Online*, 2005, **61**, o3618–o3620.